Turkish Journal of Electrical Engineering & Computer Sciences

http://journals.tubitak.gov.tr/elektrik/

Research Article

Turk J Elec Eng & Comp Sci
(2021) 29: 1643 – 1658

doi:10.3906/elk-2005-152

Analysis and simulation of efficiency optimized IPM drives in constant torque region with reduced computational burden

Mikail KOÇ[1,*], **Selçuk EMİROĞLU**[2], **Bünyamin TAMYÜREK**[3]

[1]Electrical and Electronics Engineering Department, Engineering and Architecture Faculty, Kırşehir Ahi Evran University, Kırşehir, Turkey

[2]Electrical and Electronics Engineering Department, Engineering Faculty, Sakarya University, Sakarya, Turkey

[3]Electrical and Electronics Engineering Department, Engineering Faculty, Gazi University, Ankara, Turkey

Received: 22.05.2020 • **Accepted/Published Online:** 20.01.2021 • **Final Version:** 31.05.2021

Abstract: Moving from internal combustion engine based towards electric based transportation is crucial for wide societies as they facilitate the use of green energy technologies such as wind and solar. Interior mounted permanent magnet (IPM) machines, also known as salient brushless alternating current (AC) machines, are commonly employed in traction applications as they have superior features, such as high efficiency operation, high torque, and power densities. The efficiency optimization in IPM drives is achieved by obtaining and operating at accurate and unique current angle for a certain electromagnetic torque demand. In conventional drives, the optimum current angle is obtained by online utilization of iterative techniques. However, these techniques result in increased burden on the processor. In addition, accuracy of the generated current commands, and hence, the drive efficiency may significantly reduce if the number of iterations is not adequate. More importantly, online zero divisions issue may result in instability of the drive system at certain operating points in real life experiments. This paper proposes an efficiency optimized IPM drive with smooth output torque production addressing the aforementioned issues. The optimum operating points as a function of electromagnetic torque demand are computed offline by Newton–Raphson approximation technique in the paper, and they are stored in the controller as look-up tables, which are then employed to achieve optimum efficiency operation at a wide range. The superiority of the proposed drive is validated through extensive simulation of a 4.1 kW prototype IPM machine designed and manufactured for traction applications and the results are discussed in detail. The paper also presents detailed high efficiency control analysis of permanent magnet machines and hence it would be quite insightful for new researchers on the topic.

Key words: Control of interior mounted permanent magnet (IPM) machines, interior permanent magnet synchronous motor (IPMSM), maximum torque per ampere (MTPA), efficient drives, alternating current (AC) drives

1. Introduction

The increasing use of conventional nonrenewable energy sources results in global warming and various environmental issues such as acid rains. Transportation is the dominant sector in which the energy consumption is quite high. Electric vehicles are playing an important role to the society as they facilitate the use of clean energy technologies such as solar, wind, biomass, and so on. Interior mounted permanent magnet synchronous motors are widely employed in traction applications since they have attractive features, such as high efficiency, high power density, high torque density, low noise, low rotor losses, robustness and so on. Interior mounted

*Correspondence: mkoc@ahievran.edu.tr

permanent magnet (IPM) machines have the highest torque to power ratio among all other types of machines owing to their salient poles. The saliency of the machine results in the availability of reluctance torque to be utilized for higher torque density and hence the efficiency. Advanced control techniques to achieve high efficiency operation utilizing the reluctance torque is, therefore, an important area for research [1].

Control of the IPM machines can be classified broadly into two groups based on the controlled state variables, *viz.*, field-oriented control (FOC), and direct torque control (DTC). While the phase currents are controlled for torque realization in FOC drives, the electromagnetic torque is controlled directly in DTC drives. Although direct control of the electromagnetic torque seems an advantage, one of the main drawbacks of DTC drives is that the controller relies on flux and torque observers whose performance may significantly deteriorate at low speeds [2]. In FOC drives, however, the measured phase currents are utilized for control of the electromagnetic torque eliminating the requirement for the torque and flux observers [3]. Moreover, the phase current limits can directly be posed in FOC drives. Thus, FOC drives may have better performance depending on the employed control strategy to drive the machine.

Modern AC drives can be classified into two categories based on the operating region, *viz.*, constant torque [4], and extended speed [5] regions where the DC link voltage is partly and fully utilized, respectively. Different control strategies are adopted to achieve high efficiency operation in these operating regions. It is widely known that the maximum torque per ampere (MTPA) control strategy is adopted in the constant torque region by optimizing the current angle β in Figure 1 [6]. This strategy minimizes the current magnitude for certain torque production and hence achieves the efficient operation since the iron losses has negligible influence in this region [7].

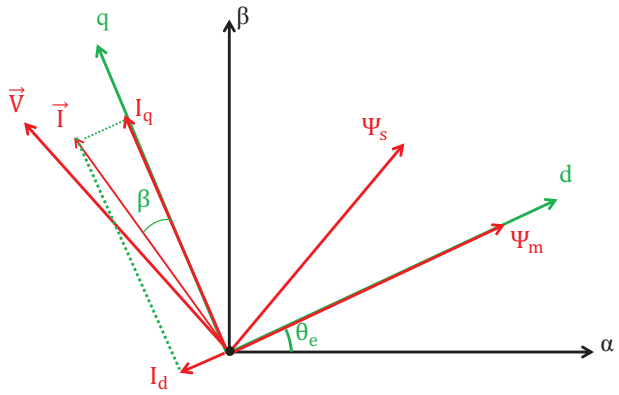

Figure 1. Current, voltage, and stator flux vectors in stationary and rotating frames.

Search algorithms are employed in [8–12] to achieve high efficiency operation in the constant torque region. The current magnitude is minimized by altering the current vector and searching for the optimum β angle. However, the search algorithm-based operation in the constant torque region may have serious problems such as poor dynamic performance due to the slow convergence rate and the reduced accuracy under disturbances. More importantly, stable operation cannot be guaranteed under rapid load variations [13].

Signal injection based MTPA control strategy has been widely researched in recent years. However, the real signal injection based techniques [13–19] suffer from increased iron and copper losses since a real signal is

injected into the current or voltage. Virtual signal injection based drives, on the other hand, suffer from model dependent operation [4, 5, 20–25].

MTPA operation can also be achieved online by employing numerical solutions [26–31]. However, in real life experiments, these solutions may significantly suffer from online zero divisions issue during computations. Additionally, increased computational burden is a serious drawback in these drives. In iteration-based drives, the burden on the processor increases as the number of iterations increases, whereas the accuracy reduces when the number of iterations reduces, and this results in reduced drive efficiency. Hence, there is a trade off between the efficiency and the computational burden. In this paper, the maximum efficiency control in the constant torque region is developed by offline utilization of Newton–Raphson approximation strategy. With this strategy, stable operation of the machine is achieved because the aforementioned issues (online zero divisions, the increase of the microprocessor burden and reduced efficiency) are handled in the drive as an offline process. The control loop calls for the commanded dq-axis current values from the preloaded tables without any delay. The effectiveness of the proposed drive is validated through sophisticated simulation of a prototype IPM machine designed for traction applications and the results are compared with the conventional drives.

2. Materials and methods

2.1. Modelling of permanent magnet machines

Clark and Park transformations of ABC frame equations give dq- axis rotating reference frame modelling of AC machines. The well-known peak convention modelling of IPM machines in the rotor reference frame are given as follows [4]:

$$\begin{bmatrix} V_d \\ V_q \end{bmatrix} = R \begin{bmatrix} I_d \\ I_q \end{bmatrix} + \frac{d}{dt} \begin{bmatrix} \Psi_d \\ \Psi_q \end{bmatrix} + \omega \begin{bmatrix} -\Psi_q \\ \Psi_d \end{bmatrix}, \tag{1}$$

$$\begin{bmatrix} \Psi_d \\ \Psi_q \end{bmatrix} = \begin{bmatrix} L_d & 0 \\ 0 & L_q \end{bmatrix} \begin{bmatrix} I_d \\ I_q \end{bmatrix} + \begin{bmatrix} \Psi_m \\ 0 \end{bmatrix}, \tag{2}$$

$$T_e = \frac{3p}{2} \left[\Psi_d I_q - \Psi_q I_d \right]. \tag{3}$$

where I_{dq}, V_{dq}, Ψ_{dq} are the rotor frame currents, voltages, and flux linkages, respectively. Ψ_m is the permanent magnet (PM) flux linkage, p is number of pole-pairs, R is the phase resistance, ω is electrical angular speed, T_e is the electromagnetic torque and L_{dq} are the dq- axis inductances, respectively. Substituting (2) into (3), one obtains the electromagnetic torque as a function of machine parameters.

$$T_e = \frac{3p}{2} \left(\Psi_m I_q - I_d I_q \left(L_q - L_d \right) \right) \tag{4}$$

As can be seen from (4), the electromagnetic torque consists of two terms, *viz.*, the permanent magnet based torque production and the reluctance torque as a result of salient poles $(L_q \neq L_d)$. The torque production in (4) can be expressed as follows:

$$T_e^{magnet} = \frac{3p}{2} \Psi_m I_q \tag{5}$$

$$T_e^{reluctance} = \frac{3p}{2} I_d I_q \left(L_d - L_q \right) \tag{6}$$

Figure 2a illustrates the magnet aligned and reluctance torque production characteristic of the prototype machine whose specifications are listed in Table 1. As seen from Figure 2a, T_e^{magnet} is maximum when β angle is zero. In addition, the reluctance torque is maximum when the angle is $45°$. It is clear that the total torque is maximized for a certain β angle between 0 and $45°$. This implies that there is a set of unique dq- axis currents to achieve high efficiency operation for a unique torque production.

The optimum β angle is obtained by posing $\partial T_e/\partial\beta$ to zero. Under the assumption of partial derivatives of machine parameters with respect to current angle is zero, the β angle is obtained as follows [32]:

$$\beta = sin^{-1}\left(\frac{-\Psi_m + \sqrt{{\Psi_m}^2 + 8\ (L_q - L_d)^2\ {I_s}^2}}{4\ (L_q - L_d)\ I_s}\right) \tag{7}$$

The dq- axis currents are given as follows as can be deduced from Figure 1.

$$\begin{aligned} I_d &= -I_s \sin\beta \\ I_q &= I_s \cos\beta \end{aligned} \tag{8}$$

Substituting (7) into (8) and solving for the d- axis current, one obtains:

$$I_d = \frac{\Psi_m}{2\ (L_q - L_d)} - \sqrt{\frac{{\Psi_m}^2}{4\ (L_q - L_d)^2} + {I_q}^2} \tag{9}$$

Utilizing (4)-(9), the optimal dq-axis current trajectory and the constant torque curves are plotted for the prototype machine in Figure 2b. Once the maximum torque per current trajectory shown in Figure 2b is achieved through the developed control strategy, then the IPM drive operates at high efficiency.

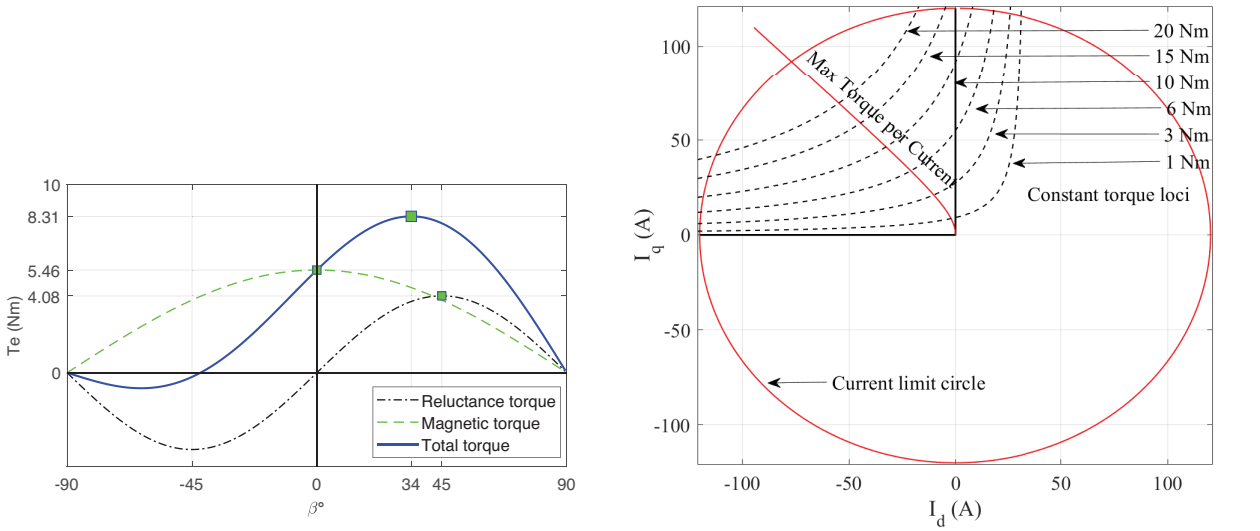

(a) Torque production of the prototype machine at 50 A.

(b) Operation area of the machine under current limit circle.

Figure 2. Torque production principle of the prototype machine.

2.2. Proposed high efficiency controlled drive system setup

The IPM machine model used in the simulated drive is obtained by employing (1)-(4) in dq- frame and its schematic is illustrated in Figure 3. By utilizing coordinate transformations (Clark/Park and their inverses) the machine modelling is transformed back into the ABC frame as in real life. It is noteworthy that the convention used in the transformations is the peak convention throughout the paper.

Figure 4 illustrates the developed drive system setup to achieve high efficiency operation for the IPM machine prototype under study. The phase currents and the rotor position are measured to achieve closed-loop control. The DC link voltage is supplied by batteries in traction applications and its level may vary between ±15% depending on the battery charge level. Hence, the DC link voltage measurement is important for traction applications. However, it should be noted that the voltage variation is not crucial in the constant torque region operation as the battery is not fully utilized in this region.

The dq-axis current errors are driven to zero through proportional integral (PI) controllers. The coupling terms in (1) are decoupled in the controller at the output of the PI controllers as shown in Figure 4. Although the drive system can still operate successfully without employing decoupling terms, their influence may increase when speed changes rapidly. The overmodulation (OM) block shown in Figure 4 is necessary to ensure that the operation is in the limitations. Otherwise, the PI controllers may generate voltage commands higher than the maximum available voltage.

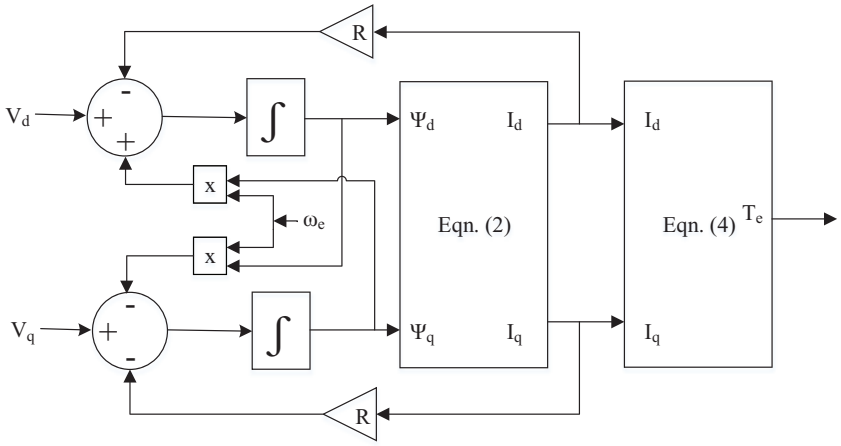

Figure 3. IPM machine modelling scheme.

Since power electronics components are utilized to apply the generated phase voltage commands to the IPM machine in real life operations, adoption of a modulation technique is a must. It is known that space vector pulse-width-modulation (SVPWM) technique is widely preferred as it facilitates higher utilization of the DC link voltage.

Input of the system is electromagnetic torque command in traction applications. Since there is only magnet alignment torque production in non-salient machines (surface mounted permanent magnet machines, $L_q = L_d$), the current command generation is quite straightforward through (5). The β angle is always zero for these machines in the constant torque region ($I_d = 0$ control). However, the challenge with the IPM machines is that there is a unique β angle for a given torque command.

Substituting (9) into (4) leads to the relationship between the electromagnetic torque and the q- axis

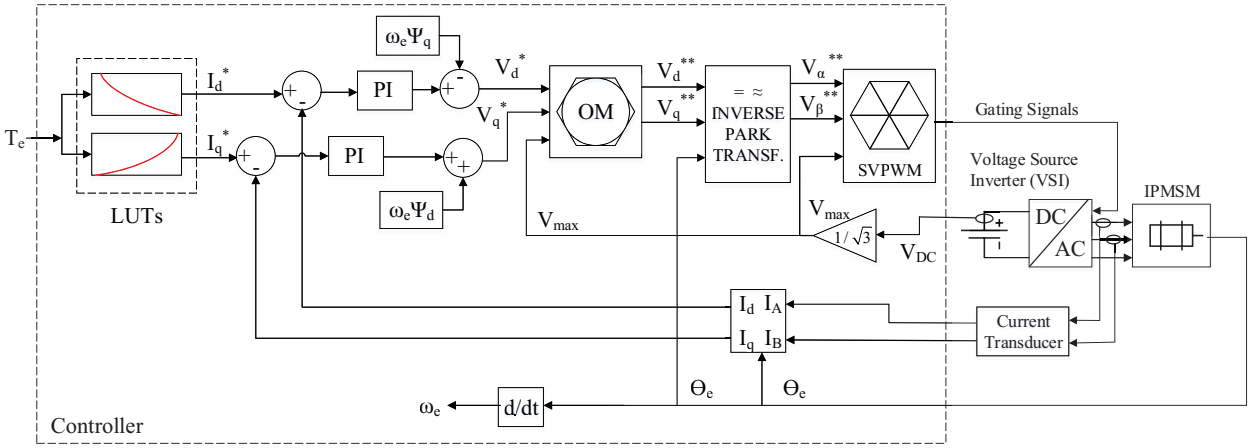

Figure 4. Schematic of the proposed drive system.

current as given by (10) where the maximum efficiency operation can be achieved in the constant torque region.

$$f\left(I_q\right) = I_q^4\left(L_d - L_q\right)^2 + I_q\frac{2T_e}{3p}\Psi_m - \left(\frac{2T_e}{3p}\right)^2 = 0 \tag{10}$$

The Newton–Raphson approximation method can be employed to solve the 4^{th} order nonlinear algebraic equation in (10) as follows:

$$I_q\left(n+1\right) = I_q\left(n\right) - \frac{f\left(I_q\left(n\right)\right)}{f\prime\left(I_q\left(n\right)\right)} \tag{11}$$

where $f\prime$ denotes the derivative of f function. The initial root values are selected as if there is no reluctance torque, and only the magnet alignment torque is produced where the current angle β is zero. Hence, the initial value of q-axis current is simply obtained by (5). It is noteworthy that the higher number of iterations is the higher accuracy in results. Once the q- axis current is obtained through several iterations, the optimal d-axis current is obtained from (9).

One can deduce from (11) that its online exploitation suffers from zero divisions issue at certain operating points since the measured currents contain harmonics in real life experiments, and this may result in instability of the drive.

The optimum dq-axis current commands for a given torque command are computed as on offline process in the proposed drive. It should be noted that experimental tests can be performed to obtain optimized dq-axis currents considering parameter variations. The dq- axis currents are stored in the controller as look-up tables (LUTs) as shown in Figure 5. Then, the control loop calls for the optimum currents from the preloaded tables without any delay. It is noteworthy that offline computation does not require experimental tests for each operating point. The table can easily be created in few seconds by a simple simulation study as long as machine parameters are known, and it can also be applied to other IPM machines as it is scalable.

Torque vs. optimum β angle, optimum currents vs. electromagnetic torque, and optimum I_q vs. I_d current to achieve high efficiency operation in the constant torque region are obtained by running the Newton–Raphson method offline and they are demonstrated in Figure 6 for the prototype machine under study.

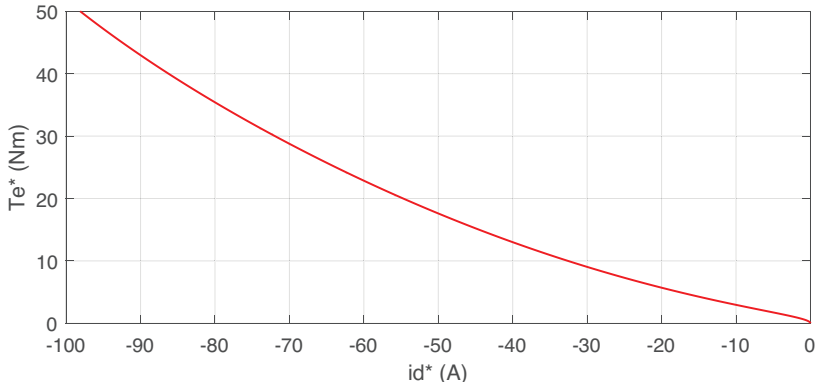

(a) Torque vs. d- axis current.

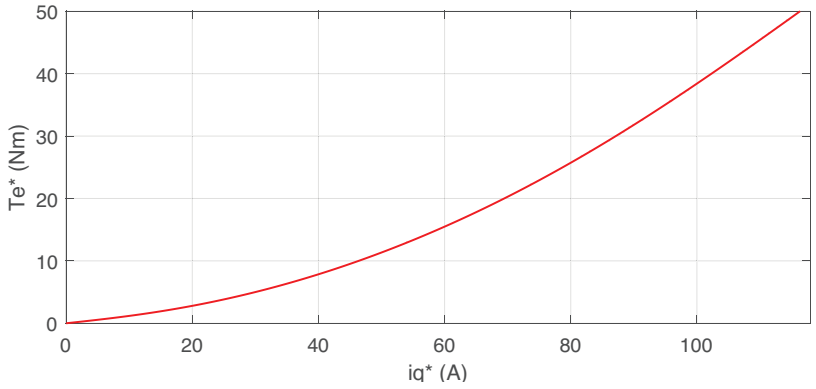

(b) Torque vs. q- axis current.

Figure 5. Optimum dq-axis current values of the prototype machine for demanded torque values.

3. Results and discussion

The proof of the control concept using parameters of a real machine is presented in this section. The prototype machine under study is shown in Figure 7 and its specifications are listed in Table 1. The motor has been designed and manufactured to verify the performance of the control systems to be developed.

3.1. Behaviour of the prototype machine under constant current magnitude operation

In this section, the drive system shown in Figure 4 is not operated with the optimum dq- axis current commands as illustrated in Figure 4 as the LUTs. Instead, a certain current magnitude command is applied to the controller as an input of the system and the β angle is varied from zero to 90° in order to see the machine and the drive behaviour for the certain current magnitude with the varying β angle. The input and the output power of the machine are expressed as (12) and (13), respectively [13].

$$P_{in} = \frac{3}{2}\left(V_d I_d + V_q I_q\right) \tag{12}$$

$$P_{out} = \omega_m T_e \tag{13}$$

where ω_m is the mechanical speed in rad/s.

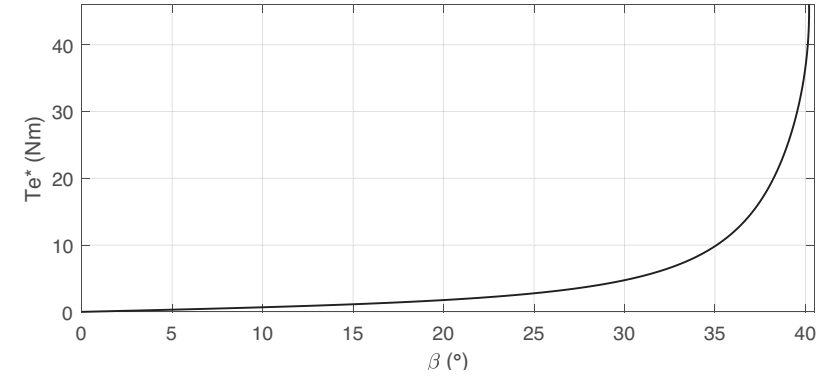

(a) Torque vs. current angle.

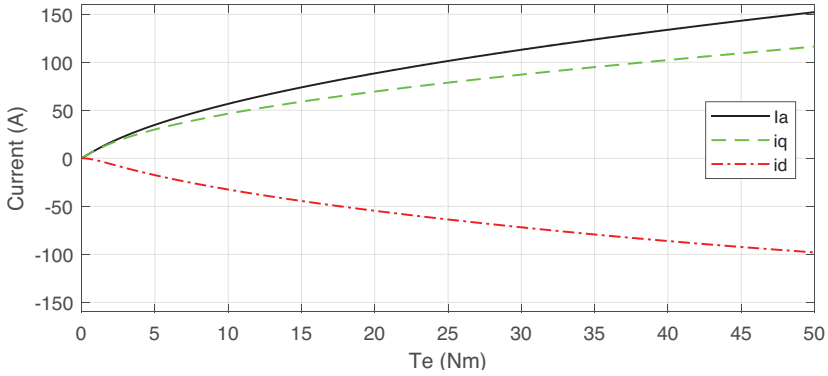

(b) Current vs. torque.

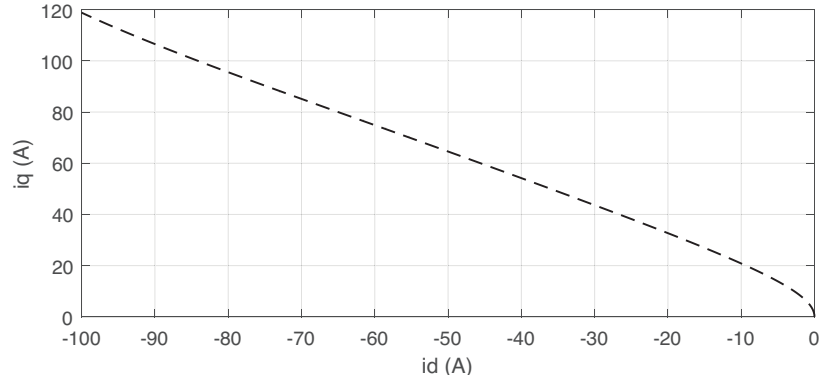

(c) q- axis current vs. d- axis current.

Figure 6. The relationship between current, torque, and β angle for the prototype machine.

The test results at 1500 rpm are demonstrated in Figure 8. The drive system is operated for every 10 A up to 100 A. The electromagnetic torque production for given current magnitude vs. β angle variation is illustrated first. Then, output power of the machine vs. β angle, electromagnetic torque production vs. d-axis current, and the machine efficiency vs. β angle for certain current magnitude operations are illustrated, respectively.

One can deduce from Figure 8 that there is a unique maximum efficiency operation point for a given

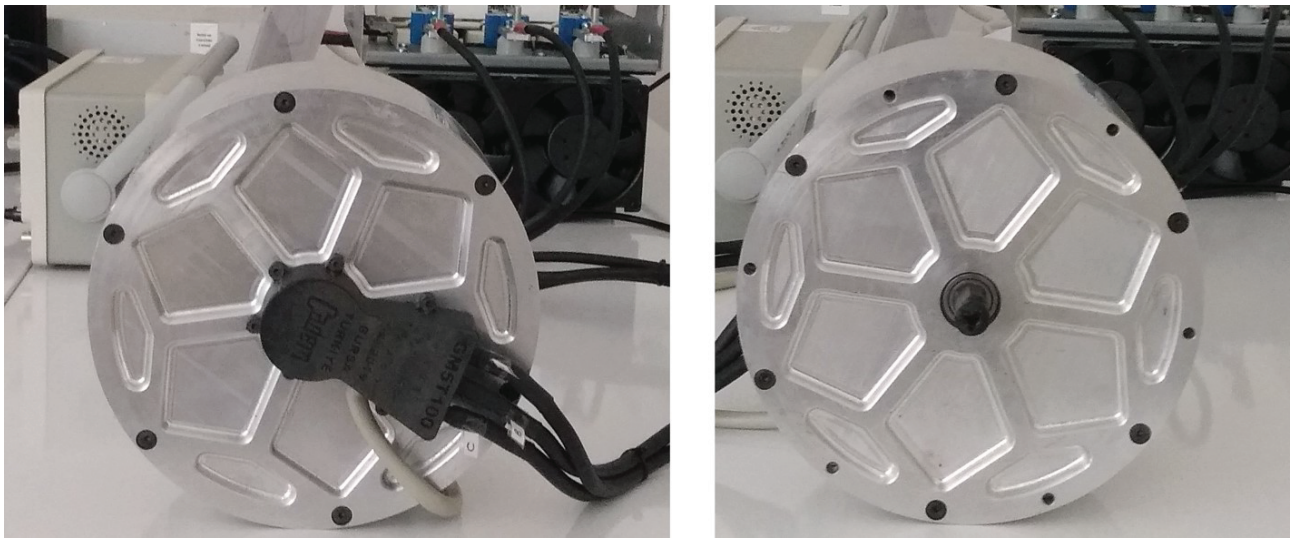

Figure 7. Front and rear views of the prototype IPM machine.

Table 1. Specifications of the prototype IPM machine.

Type	Interior Mounted Permanent Magnet Synchronous Machine	
Number of phase / poles	3/8	
Nominal Speed	2500 RPM	@120 V DC
Continuous Torque	15.7 Nm	@51.6 Arms
Continuous Power	4.1 kW	@120 V DC
Input Voltage Range	12 V – 600 V	
Nominal d- Axis Inductance	0.282 mH	
Nominal q- Axis Inductance	0.827 mH	
Nominal PM Flux Linkage	0.0182 Wb	
Nominal Phase Resistance	0.0463 Ω	
Inertia	0.0072 kgm^2	
Position Sensor	Encoder:Absolute position SPI output + 8192 ppr incremental (ABZ) output	

current command. At this point, the electromagnetic torque production for certain current magnitude is maximized and, accordingly, the output power and the efficiency become maximum. In Figure 8, while the maximum electromagnetic torque production at 50 A current magnitude at $\beta = 34°$ is 8.31 Nm for the prototype machine, it would be 5.46 Nm at $\beta = 0°$ if the reluctance torque is not utilized ($I_d = 0$ control). This perfectly matches with the torque production in Figure 2a. In addition, motor efficiency reduces as the current magnitude increases at certain speed. This is as expected since the copper losses (I^2R losses) increase with the increasing current magnitude and hence the efficiency reduces. Similarly, the increase of phase resistance in real life experiments will reduce the efficiency of the motor and vice versa. However, it is important to note that the optimum operating point for MTPA control is not influenced by the resistance variations as

the torque maximization is exempt from resistance value based on (4). It should be noted that the operating points utilizing (7) gives optimum results since parameters do not vary with β angle in the drive.

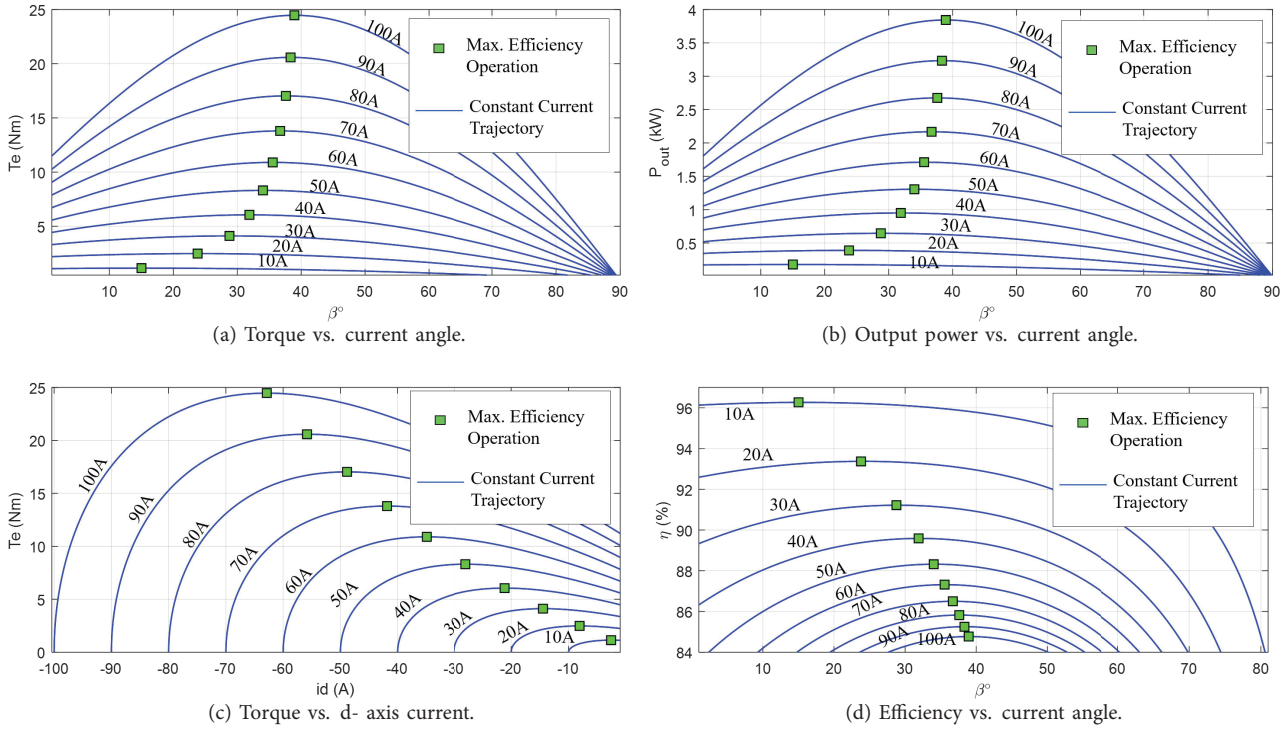

(a) Torque vs. current angle.

(b) Output power vs. current angle.

(c) Torque vs. d- axis current.

(d) Efficiency vs. current angle.

Figure 8. Constant current magnitude operation results.

3.2. Validation of the issues pertinent to online iteration based control techniques

As it has been discussed previously in the paper, the number of iterations needs to be sufficient to obtain high efficiency operation points in conventional online iteration-based drives. Figure 9 illustrates the influence of the number of iterations on the resultant operating point of the prototype IPM machine when it rotates at 500 rpm mechanical speed. As seen from Figure 9, since all points are on the constant torque production curve, the machine produces the demanded 25 Nm electromagnetic torque at any operating point regardless of the number of iterations. Hence, the machine speed and the output torque production are the same at these points. This implies that the output power at any operating point shown in Figure 9 are the same based on (13). However, it is clear from Figure 9b that the input power associated with each operating point is not the same and show significant differences in power absorption from the grid (or battery in electric vehicles) when the number of iterations varies. This results in reduced drive efficiency when the accurate dq- axis current commands are not generated due to insufficient iteration. More importantly, the controller may generate current commands outside the current limit circle when the number of iterations is less. Current limit may be posed to protect the machine, but the machine will not produce the demanded torque in this case.

Although the increase of the online iteration number increases the accuracy and hence the drive efficiency, the burden on the processor comes out as a drawback in this case since the processor will always be computing even at steady states. To validate the burden issue of the online iterative techniques, the drives with and

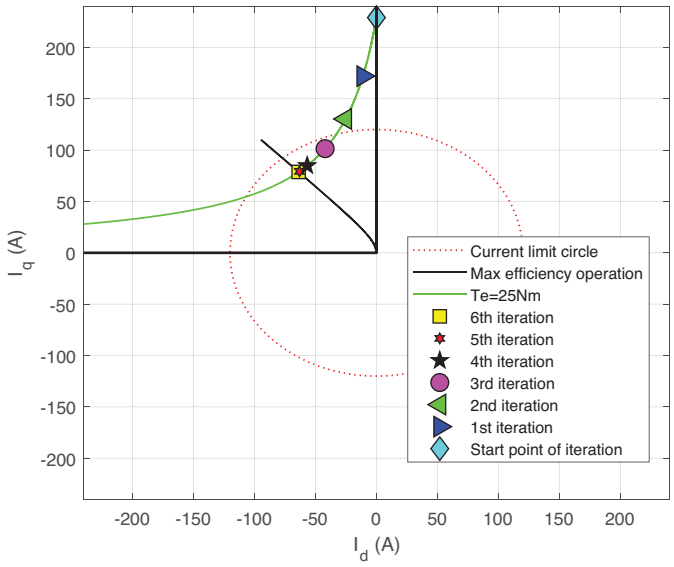

(a) Operating points versus number of iterations.

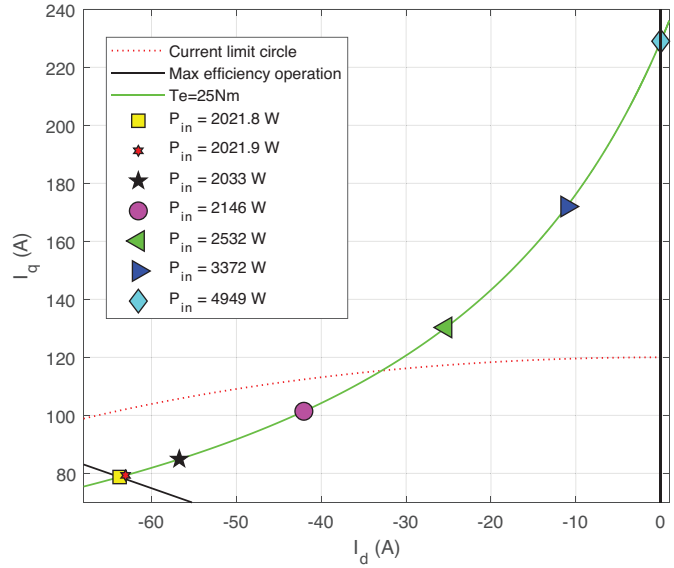

(b) Zoom of a.

Figure 9. Issues pertinent to online iteration-based techniques.

without online iterations are simulated with the same torque and speed profile as shown in Figure 10a. For a fair comparison, identical drives were employed except for the LUTs part shown in Figure 4. Reference current command generation in conventional drives only include the online iteration strategy given by (11) and do not include any irrelevant element to increase the computational burden unnecessarily. The drives have been simulated on a PC with i5 CPU and 3 GHz processor, and time durations to simulate the given profile are shown in Figure 10b. It is evident that the computational burden increases drastically as the number of iterations

increases and the proposed drive has the lowest burden since it achieves the quickest simulation.

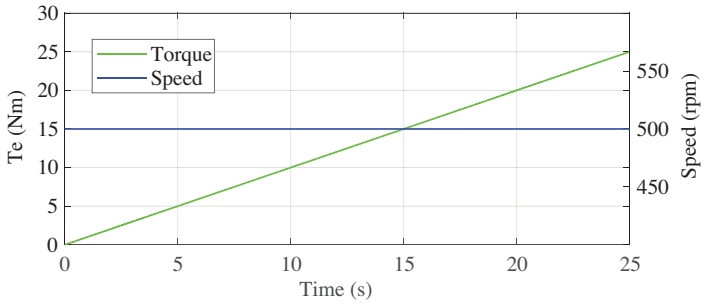

(a) Operation profile of each drive.

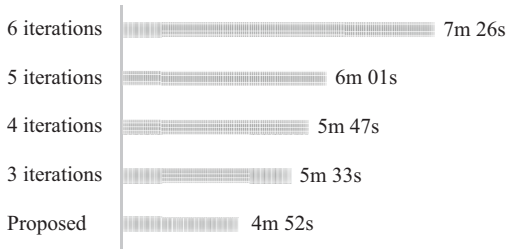

(b) Time duration of each drive to simulate the given profile.

Figure 10. Comparisons of processor burden.

3.3. Proposed maximum efficiency control validation

In this section, the drive system shown in Figure 4 is operated with the optimum dq- axis current commands generated by the LUTs. The system input is electromagnetic torque command and the drive operates at the maximum efficiency operation points shown in Figure 8. The machine is operated for given torque and speed profile as illustrated in Figure 11. The reference and actual values of the electromagnetic torque and dq- axis currents as well as the electrical operating frequency of the machine, input and output powers, efficiency, current magnitude, β angle, phase currents in ABC frame, operating voltage magnitude and the maximum available voltage are all illustrated in Figure 11.

It is noteworthy that a low-pass filter is employed before the speed and the electromagnetic torque command since the step responses are not desired in traction applications for comfort of the passengers. The remarks that should be noted for the results may be listed as follows:

- The actual values of the variables track the references quite well without any overshoot and remarkable delay.
- For the given torque commands, the optimum phase current commands are generated from the LUTs without any delay, and hence, the current magnitude to achieve the given torque production is minimized, ie. maximum efficiency control.
- 10 Nm torque is achieved when current magnitude, β angle, and dq- axis currents are nearly 58 A, 35°, -32 A and 46 A, respectively. One can deduce that these operating points match well with Figure 5, Figure 6, and Figure 8.
- Electrical frequency of the machine is proportional to the speed and the variations of the frequency can be observed from the phase currents in ABC frame.
- While the voltage magnitude is slightly influenced by the electromagnetic torque, the DC link voltage utilization increases with the speed.
- The DC link voltage is partly utilized in the constant torque region.

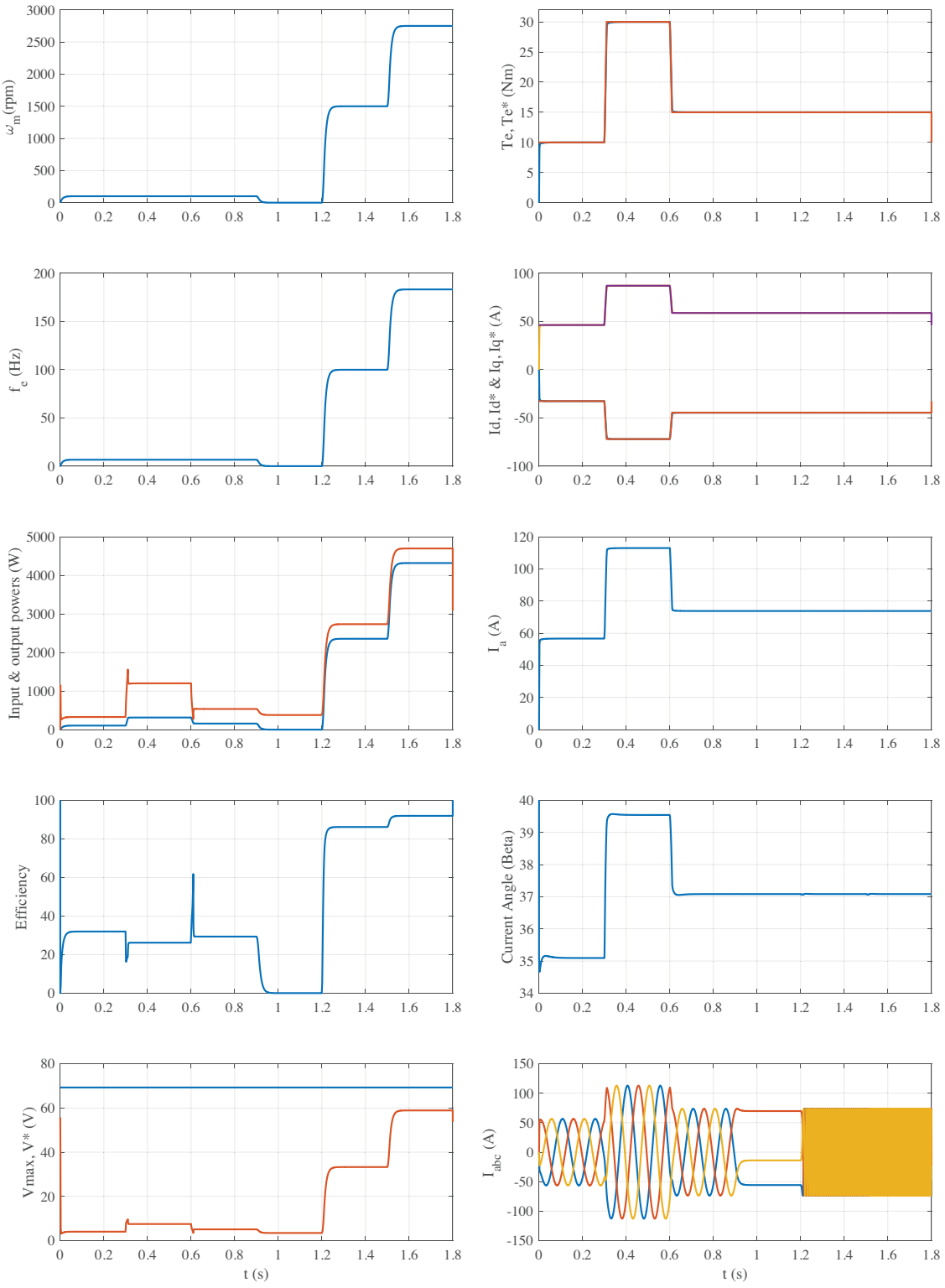

Figure 11. Proposed drive system results.

- The machine is able to operate even at zero speed whereas a large number of drive systems in the literature is not able to operate at standstill, and the efficiency at this operating point is zero as expected since the output power is zero (13).

4. Conclusion

In this paper, a maximum efficiency control in the constant torque region is adopted for a 4.1 kW prototype IPM machine designed for traction applications. To achieve the maximum efficiency, the optimal dq- axis currents are computed offline as a function of electromagnetic torque and stored in the controller as LUTs. The Newton-Raphson approximation method has been employed to obtain the optimal currents offline for the ease of computation. By doing so, the burden on the processor is reduced significantly and the online zero divisions issue in the controller is handled. In addition, implementation of the strategy for other IPM machines is straightforward as long as machine parameters are known. The proposed drive system has been tested under different operating points and the results on a prototype machine validate its superiority comparing the conventional drives.

Acknowledgment

This study has been supported by the Scientific and Technological Research Council of Turkey (TUBITAK) through the Scientific and Technological Research Projects Funding Program (1001) with a project numbered as 118E858.

References

[1] Li H, Qian Y, Asgarpoor S, Sharif H. Simulation study on on-line MTPA/MTPV trajectory tracking in PMSMs with power management. Electric Power Components and Systems 2020; 48 (3): 241-255. doi: 10.1080/15325008.2020.1758849.

[2] Koc M, Wang J, Sun T. Stator flux oriented control for high performance interior permanent magnet synchronous machine drives. In: 8th IET International Conference on Power Electronics, Machines and Drives (PEMD 2016); Glasgow, UK: 2016. pp. 1-6.

[3] Lai C, Feng G, Tjong J, Kar N C. Direct calculation of Maximum-Torque-per-Ampere angle for interior PMSM control using measured speed harmonic. IEEE Transactions on Power Electronics 2018; 33 (11): 9744-9752. doi: 10.1109/TPEL.2017.2789245.

[4] Sun T, Wang J, Chen X. Maximum Torque Per Ampere (MTPA) Control for Interior Permanent Magnet Synchronous Machine Drives Based on Virtual Signal Injection. IEEE Transactions on Power Electronics 2015; 30 (9): 5036-5045.doi: 10.1109/TPEL.2014.2365814.

[5] Sun TF, Wang JB. Extension of virtual-signal-injection-based MTPA control for Interior Permanent-Magnet Synchronous Machine drives into the field-weakening region. IEEE Transactions on Industrial Electronics 2015; 62 (11): 6809-6817. doi: 10.1109/TIE.2015.2438772.

[6] Huyn TA, Hsieh MF. Comparative study of PM-Assisted SynRM and IPMSM on constant power speed range for EV applications. IEEE Transactions on Magnetics 2017; 53 (11): 1-6. doi: 10.1109/TMAG.2017.2707125.

[7] Araz HK, Yılmaz M. Design procedure and implementation of a high-efficiency PMSM with reduced magnet-mass and torque-ripple for electric vehicles. Journal of the Faculty of Engineering and Architecture of Gazi University 2020; 35 (2): 1089-1109. doi: 10.17341/gazimmfd.458515.

[8] Colby RS, Novotny DW. An efficiency-optimizing permanent-magnet synchronous motor drive. IEEE Transactions on Industry Applications 1988; 24 (3): 462-469. doi: 10.1109/28.2897.

[9] Dianov A, Young-Kwan K, Sang-Joon L, Sang-Taek L. Robust self-tuning MTPA algorithm for IPMSM drives. In: IECON 2008 34th Annual Conference of IEEE Industrial Electronics; Orlando, FL, USA; 2008. pp. 1355-1360. doi: 10.1109/IECON.2008.4758151.

[10] Lee KW, Lee SB. MTPA operating point tracking control scheme for vector controlled PMSM drives. In: International Symposium on Power Electronics, Electrical Drives, Automation and Motion, SPEEDAM; Pisa, Italy; 2010. pp. 24-28. doi: 10.1109/SPEEDAM.2010.5544955.

[11] Ahmed A, Sozer Y, Hamdan M. Maximum torque per ampere control for interior permanent magnet motors using DC link power measurement. In: 2014 IEEE Applied Power Electronics Conference and Exposition - APEC 2014; Fort Worth, TX, USA; 2014. pp. 826-832. doi: 10.1109/APEC.2014.6803403.

[12] Zhu ZQ, Chen YS, Howe D. Online optimal flux-weakening control of permanent-magnet brushless AC drives. IEEE Transactions on Industry Applications 2000; 36 (6): 1661-1668. doi: 10.1109/28.887219.

[13] Sungmin K, Yoon Y, Sul S, Ide K. Maximum Torque per Ampere (MTPA) control of an IPM machine based on signal injection considering inductance saturation. IEEE Transactions on Power Electronics 2013; 28 (1): 488-497. doi: 10.1109/TPEL.2012.2195203.

[14] Tan Y, Moase WH, Manzie C, Nešić D, Mareels IMY. Extremum seeking from 1922 to 2010. In: Proceedings of the 29th Chinese Control Conference; Beijing, China; 2010. pp. 14-26.

[15] Bolognani S, Peretti L, Zigliotto M. Online MTPA control strategy for DTC Synchronous-Reluctance-Motor drives. IEEE Transactions on Power Electronics 2011; 26 (1): 20-28. doi: 10.1109/TPEL.2010.2050493.

[16] Bolognani S, Petrella R, Prearo A, Sgarbossa L. Automatic tracking of MTPA trajectory in IPM motor drives based on AC current injection. IEEE Transactions on Industry Applications 2011; 47 (1): 105-114. doi: 10.1109/ECCE.2009.5316066.

[17] Antonello R, Carraro M, Zigliotto M. Towards the automatic tuning of MTPA algorithms for IPM motor drives. In: 2012 XXth International Conference on Electrical Machines (ICEM); Marseille, France; 2012. pp. 1121-1127. doi: 10.1109/ICElMach.2012.6350016.

[18] Antonello R, Carraro M, Zigliotto M. Theory and implementation of a MTPA tracking controller for anisotropic PM motor drives. In IECON 2012 - 38th Annual Conference on IEEE Industrial Electronics Society; Montreal, QC, Canada; 2012. pp. 2061-2066 doi: 10.1109/IECON.2012.6388741.

[19] Antonello R, Carraro M, Zigliotto M. Maximum-Torque-Per-Ampere operation of anisotropic synchronous permanent-magnet motors based on extremum seeking control. IEEE Transactions on Industrial Electronics 2014; 61 (9): 5086-5093. doi: 10.1109/TIE.2013.2278518.

[20] Sun T, Wang J, Koc M, Chen X. Self-Learning MTPA control of interior permanent magnet synchronous machine drives based on virtual signal injection. IEEE Transactions on Industry Applications 2016; 52 (4): 3062-3070. doi: 10.1109/TIA.2016.2533601.

[21] Sun T, Wang J, Koc M. Virtual signal injection based direct flux vector control of IPMSM drives. IEEE Transactions on Industrial Electronics 2016; 63 (8): 4773-4782. doi: 10.1109/TIE.2016.2548978.

[22] Sun T, Wang J, Koc M, Chen X. Self-Learning MTPA control of interior permanent magnet synchronous machine drives based on virtual signal injection. In: 2015 IEEE International Electric Machines and Drives Conference (IEMDC); Coeur d'Alene, ID, USA; 2015. pp. 1056-1062. doi: 10.1109/IEMDC.2015.7409192.

[23] Li M, Huang S, Wu X, Liu K, Peng X, Liang G. A virtual HF signal injection based maximum efficiency per ampere tracking control for IPMSM drive. IEEE Transactions on Power Electronics 2020; 35 (6): 6102-6113. doi: 10.1109/TPEL.2019.2951754.

[24] Chen Z, Yan Y, Shi T, Gu X, Wang Z, Xia C. An accurate cirtual signal injection control for IPMSM with improved torque output and widen speed region. IEEE Transactions on Power Electronics 2020; 36 (2): 1941-1953. doi: 10.1109/TPEL.2020.3010300.

[25] Zhang W, Xiao F, Liu J, Mai Z, Li C. Maximum torque per ampere control for IPMSM traction system based on current angle signal injection method. Journal of Electrical Engineering & Technology 2020; 15 (4): 1681-1691. doi: 10.1007/s42835-020-00434-5.

[26] Hoang KD, Wang J, Cyriacks M, Melkonyan A, Kriegel K. Feed-forward torque control of interior permanent magnet brushless AC drive for traction applications. In: 2013 IEEE International Electric Machines & Drives Conference (IEMDC); Chicago, IL, USA; 2013. pp. 152-159. doi: 10.1109/IEMDC.2013.6556247.

[27] Yu-Seok J, Sul S, Hiti S, Rahman KM. Online minimum-copper-loss control of an interior permanent-magnet synchronous machine for automotive applications. IEEE Transactions on Industry Applications 2006; 42 (5): 1222-1229. doi: 10.1109/TIA.2006.880910.

[28] Hoang KD, Zhu ZQ, Foster M. Online optimized stator flux reference approximation for maximum torque per ampere operation of interior permanent magnet machine drive under direct torque control. In: 6th IET International Conference on Power Electronics, Machines and Drives (PEMD 2012); Bristol, UK; 2012. pp. 1-6. doi: 10.1049/cp.2012.0266.

[29] Khoa DH, Aorith HKA. Online control of IPMSM drives for traction applications considering machine parameter and inverter nonlinearities. IEEE Transactions on Transportation Electrification 2015; 1 (4): 312-325. doi: 10.1109/TTE.2015.2477469.

[30] Hang J, Wu H, Ding S, Huang Y, Hua W. Improved loss minimization control for IPMSM using equivalent conversion method. IEEE Transactions on Power Electronics 2021; 36 (2): 1931-1940. doi: 10.1109/TPEL.2020.3012018.

[31] Choi K, Kim Y, Kim K. Real-time optimal torque control of interior permanent magnet synchronous motors based on a numerical optimization technique. IEEE Transactions on Control Systems Technology 2020; 1-8. doi: 10.1109/TCST.2020.3006900.

[32] Sun T, Koç M, Wang J. MTPA control of IPMSM drives based on virtual signal injection considering machine parameter variations. IEEE Transactions on Industrial Electronics 2018; 65 (8): 6089-6098. doi: 10.1109/TIE.2017.2784409.